Colloid Polym Sci (2005) 283: 1313–1320
DOI 10.1007/s00396-005-1345-y

ORIGINAL CONTRIBUTION

**Caroline A. Ericsson**
**Olle Söderman**
**Stefan Ulvenlund**

# Aggregate morphology and flow behaviour of micellar alkylglycoside solutions

Received: 17 January 2005
Accepted: 15 April 2005
Published online: 5 July 2005


C. A. Ericsson · O. Söderman
S. Ulvenlund (✉)
Department of Physical Chemistry 1,
Centre of Chemistry and Chemical
Engineering, Lund University,
P.O. Box 124, 22100 Lund, Sweden
E-mail: stefan.ulvenlund@astrazeneca.com
Tel.: +46-46-337847
Fax: +46-46-337128

S. Ulvenlund
AstraZeneca R & D Lund,
22187 Lund, Sweden

**Abstract** Solutions of *n*-nonyl-β-D-glucoside ($C_9G_1$), *n*-decyl-β-D-glucoside ($C_{10}G_1$), *n*-dodecyl-β-D-maltoside ($C_{12}G_2$), *n*-tetradecyl-β-D-maltoside ($C_{14}G_2$) and $C_9G_1/C_{10}G_1$ mixtures have been characterised by capillary viscometry and rheology in $H_2O$ and $D_2O$, in order to map the influence of surfactant characteristics on micellisation over a wide concentration range. For the maltosides, the micellar solutions are shear thinning with a zero-shear viscosity that scales with concentration according to a power law with an exponent of about 5.8. In contrast, solutions of the glucosides $C_9G_1$, $C_{10}G_1$ and their mixtures show Newtonian flow behaviour and a much lower scaling exponent ($< 2.4$). In $C_9G_1/C_{10}G_1$ mixtures, the scaling exponent decreases monotonously with increasing $C_{10}G_1$ content. The flow behaviour correlates with the packing requirements of the various surfactants, and are compatible with the idea that the maltosides form worm-like micelles, whereas the glucosides form branched, interconnected micelles ($C_9G_1$) and space-filling micellar networks ($C_{10}G_1$).

**Keywords** Alkylglycosides · Rheology · Surfactant solution · Micellar network · Deuterium isotope effect

## Introduction

Surfactants in aqueous media self-assemble to form aggregates at a specific concentration known as the critical micelle concentration (cmc). The aggregates formed are often spherical or quasi-spherical in shape, but may undergo dramatic growth as a result of a change of a suitable "tuning parameter". This parameter may be salt concentration, temperature or concentration of an additive (e.g. a fatty alcohol). The process of micellar growth results in the formation of worm-like or branched micelles, or even interconnected micellar networks. Micellar growth, and the dynamic properties of systems comprising large micelles, has been extensively studied for ionic surfactants, where the growth is normally induced by increasing the electrolyte concentration. Well-studied examples include the cetylpyridinium chlorate/sodium chlorate [1–3], cetyltrimethylammonium bromide/potassium bromide [3–6], and cetylpyridinium chloride/sodium salicylate systems [7–9]. Upon increasing salt concentration, the viscometric behaviour of these systems have been interpreted in terms of formation of a network of worm-like micelles ("living polymers"), followed by formation of branched aggregates [3, 7, 10, 11]. In such branched aggregates, stress relaxation can occur by sliding the cross-links along the worm-like micelles, which gives rise to a decrease in viscosity [12].

The literature on the properties of worm-like micelles of non-ionic surfactants is less extensive. However, surfactants based on polyethyleneoxide are known to undergo a sphere-to-rod transition when the temperature or concentration is increased. Entangled networks of worm-like micelles have been found to form at concentration above the overlap concentration [13, 14], whereas formation of branched aggregates has been

claimed to form only in the vicinity of the lower critical consolute temperature [13, 15].

Alkylglycosides represent a class of non-ionic surfactants whose rheological behaviour in aqueous solution is less studied [16, 17]. Alkylglycosides have been suggested to form elongated micellar structures of several kinds, which clearly make them interesting from a rheological point of view. Nonylglucoside ($C_9G_1$) and decylglucoside ($C_{10}G_1$) have both been shown to form large micelles over a wide concentration range [18, 19]. However, the phase behaviour of the two surfactants suggests important differences in micellisation [18]. At room temperature, $C_9G_1$ displays a large micellar region in water, which upon increasing concentration is followed by a bicontinuous cubic phase with the space group *Ia3d*. NMR self-diffusion data suggest that the microstructure in the micellar and cubic phases is similar [18]. $C_{10}G_1$, on the other hand, displays phase separation at concentrations between 0.1 wt% and 17 wt%. Above 17 wt% a one-phase micellar region is present, which extends up to approximately 67 wt% [18]. Characterisation of the more concentrated phases have been hampered by kinetic effects, although hexagonal, cubic and lamellar phases have been reported [16]. NMR data indicate that the microstructure of the micellar phase in the $C_9G_1/D_2O$ and $C_{10}G_1/D_2O$ systems is similar and the data also suggest that this structure is best described in terms of a multi-connected micellar network [18]. The implied, close similarities in micellar morphology between the two systems would seem to contradict the pronounced differences in phase behaviour in the micellar domain. This has been explained by assuming that $C_{10}G_1$ forms a near-saturated network, whereas $C_9G_1$ forms micelles that are highly branched and interconnected, but nevertheless containing a large enough number of end-points to allow for dilution without phase separation [20]. Similarly, the entire micellar region of the ternary phase diagram of $C_9G_1/C_{10}G_1/H_2O$ has been suggested to comprise a network of branched micelles in which the relative number of end-points increases with the amount of $C_9G_1$ [20–22].

Understanding of alkylmaltoside micelle morphology seems less well-developed, particularly for higher concentrations. *n*-Tetradecyl-*β*-D-maltoside ($C_{14}G_2$) has been shown to form worm-like micelles already at low concentrations [23], but shorter-chain maltosides seem to form smaller micelles under dilute conditions [24, 25]. The phase behaviour of alkylmaltosides suggests that they rarely form branched aggregates. The phase diagrams of $C_8G_2$, $C_{10}G_2$ and $C_{12}G_2$ have been published [26, 27]. All three surfactants have a high solubility in water, which results in a wide micellar domain in which no phase separation is observed. At higher surfactant concentrations, hexagonal, rectangular, cubic and lamellar phases have been characterised. The phase diagram of $C_{14}G_2$ has not been published, but probably resembles that of $C_{12}G_2$.

The micellar morphology of both alkylglucosides and alkylmaltosides has been shown to display anomalous deuterium effects. In the $C_9G_1$ and $C_{14}G_2$ systems, substituting $D_2O$ for $H_2O$ leads to a quite dramatic increase in micelle size, even at low concentrations [19, 23]. Similarly, the 2-phase loop in the $C_9G_1/C_{10}G_1/D_2O$ system is much larger than in the $C_9G_1/C_{10}G_1/H_2O$ one at otherwise similar conditions [28].

In summary, available literature data suggest that alkylglycosides form an unusually wide array of micellar morphologies. However, the assignment of morphologies is, in the maltoside cases, based largely on analogies with the phase behaviour and extrapolation from dilute conditions. Similarly, the understanding of the deuterium effect on micelle morphologies is incomplete and the details of micellar network formation in alkylglucosides need to be verified.

In the present work, we have used viscometry and rheology to investigate the effects of alkylglycoside molecular characteristics (primarily packing requirements) on micellar morphology over a wide concentration range. The results shed further light on the general differences in micellisation between glucosides and maltosides at high surfactant concentration.

## Materials and methods

### Materials and sample preparation

*n*-Nonyl-*β*-D-glucoside ($C_9G_1$), *n*-decyl-*β*-D-glucoside ($C_{10}G_1$), *n*-dodecyl-*β*-D-maltoside ($C_{12}G_2$) and *n*-tetradecyl-*β*-D-maltoside ($C_{14}G_2$) were purchased from Anatrace Inc. (Maumee, OH) and was of ANAGRADE quality. $H_2O$ was distilled and further purified on a PureLab Plus water purification apparatus and filtered through a 0.10 μm filter. $D_2O$ with an isotopic purity of 99% was purchased from Cambridge Isotope Laboratories.

### Calculation of concentration and volume fraction

All concentrations are given in wt%. Volume fractions can be estimated from the surfactant densities. The density can be calculated by using the volume of the surfactant molecule, which has been determined to 691 $Å^3$ for $C_{12}G_2$ [24]. However, this value provides an underestimate of the molecular volume in solution, since the hydrophilic head-group in this case also includes water of hydration. Taking hydration into account yields a molecular volume of 991 $Å^3$ for the same surfactant, assuming ten water molecules with a volume of 30 $Å^3$ each per surfactant molecule [24]. From these

molecular volumes the density of $C_{12}G_2$ with and without water of hydration can be calculated as 1.16 g/cm$^3$ and 1.23 g/cm$^3$, respectively. Using the same calculation in conjunction with the assumption that the density of the alkyl chain is that of the corresponding liquid alkane gives a density of $C_{14}G_2$ of 1.14 g/cm$^3$ (with ten waters of hydration) and 1.20 g/cm$^3$ (without water of hydration). The same type of calculation was applied to the alkylglucosides, $C_9G_1$ and $C_{10}G_1$. The head-group volume for $C_8G_1$ has been determined to 179.4 Å$^3$ [25], which gives a calculated density of 1.13 g/cm$^3$ for $C_9G_1$ and 1.12 g/cm$^3$ for $C_{10}G_1$, without water of hydration. The observation that the estimated density of all surfactants is close to 1, regardless of assumptions, leads to the trivial conclusion that the weight concentration is approximately equal to the volume fraction, $\phi$, for the alkylglycoside systems.

In mixtures of $C_9G_1$ and $C_{10}G_1$, $\delta$ denotes the mass ratio of $C_9G_1$ defined as

$$\delta = \frac{m_{C_9G_1}}{m_{C_9G_1} + m_{C_{10}G_1}}. \quad (1)$$

## Methods

The capillary viscometers were of Cannon-Fenske type and fitted in a mantle through which thermostatted water was circulated by means of an external water bath. The specific constants ($K$) of the capillaries were in the range 0.00381–0.2150 mm$^2$/s$^2$. In a given experiment, the capillary was selected so as to give a flow-through time of $>200$ s. Densities of solutions were determined by repeated weighing of the solutions in a volumetric flask. The flask was calibrated by weighing of water at 22 °C.

Rheological experiments were performed on a Reologica Stress Tech using a cone-plate geometry with a diameter of 40 mm and a cone angle of 4 ° (CP 40–4). A solvent trap was used to prevent evaporation of water. The samples were thermostatted at 22 °C by a circulating water bath for all the surfactants except $C_{10}G_1$ and $C_{14}G_2$ which were investigated at 25 and 35 °C respectively, in order for the measurements to be performed above the Krafft temperature (32 °C for $C_{14}G_2$ and 23 °C for $C_{10}G_1$). In oscillatory experiments, the frequency range investigated was 0.1 Hz $\leq f \leq$ 15 Hz. In flow-curve experiments, the shear-rate range was $0.15\,s^{-1} \leq \dot{\gamma} \leq 3030\,s^{-1}$.

## Theoretical concepts

An extensive theoretical treatment of the dynamics and rheology of worm-like micelles (“living polymers”) has been presented by Cates [29, 30]. Here, we limit ourselves to a brief summary of the theoretical concepts required to discuss and rationalise the experiments in the present paper. The Cates model involves two time scales, namely the reptation time $\tau_{rep}$ and the breaking time $\tau_{br}$ of the micelles [29]. In the limit of $\tau_{rep} \ll \tau_{br}$, micellar scission and reformation do not significantly affect the stress relaxation. In combination with the predictions of mean-field theory [31], these conditions give

$$\eta_0 \sim \phi^{21/4}, \quad (2)$$

where $\phi$ is the volume fraction of surfactant. For the other extreme case, where $\tau_{rep} \gg \tau_{br}$, the viscosity is predicted to scale with the volume fraction of the surfactant solution as

$$\eta_0 \sim \phi^{7/2}. \quad (3)$$

In Cates model, an exponent lower than 3.5 can be accounted for if the distance between entanglement points is assumed much larger than the persistence length and the breaking time is much larger than the Rouse time [32]. However, the model predicts that the scaling exponent for an entangled system cannot be lower than 2.0, irrespective of relaxation mechanism and relaxation time.

Formation of micellar branch points and thus of inter-micellar cross-links makes the situation much more complex. Cross-linked micellar systems (“living networks”) have been discussed from a theoretical point of view by Drye, Cates and Lequeux [12, 33], but the fundamental understanding of such systems is still less extensive than for entangled ones. Nevertheless, the scaling exponent is expected to be lower than 3.5.

## Results and discussion

### Dodecyl- and tetradecylmaltoside, $C_{12}G_2$ and $C_{14}G_2$

The viscosity of $C_{14}G_2$ solutions as a function of shear rate was investigated in $D_2O$ and $H_2O$ (Fig. 1). The data reveal that $C_{14}G_2$ solutions display Newtonian behaviour at low shear rates and pronounced shear thinning at high shear rates. At high surfactant concentration the Newtonian viscosity of solutions in $D_2O$ is roughly one order of magnitude higher than those in $H_2O$.

Concentrated $C_{14}G_2$ solutions display a viscoelastic behaviour with a characteristic time of approximately 0.17 s (Fig. 2). As illustrated in Fig. 2, the frequency dependence of the $C_{14}G_2$ system does not follow the Maxwell model. However, a similar non-Maxwellian rheological behaviour has been observed in mixtures of cetylpyridinium chloride and sodium salicylate at low and moderate concentrations of salicylate [7]. These systems comprise worm-like, non-branched micelles and the fact that the Maxwell model is unable to describe

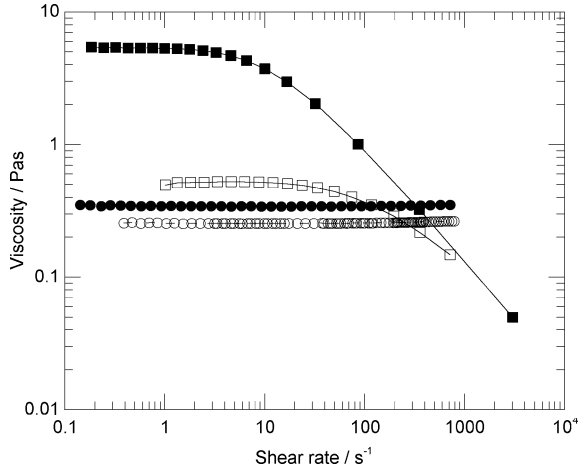


**Fig. 1** Flow curves (viscosity as a function of shear rate, $\dot{\gamma}$) for 20.0 wt% $C_{14}G_2$ in $H_2O$ (*open squares*), 18.5 wt% $C_{14}G_2$ in $D_2O$ (*filled squares*), 42.5 wt% $C_9G_1$ in $H_2O$ (*open circles*) and 42.4 wt% $C_9G_1$ in $D_2O$ (*filled circles*). The *lines* are included as a guide to the eye

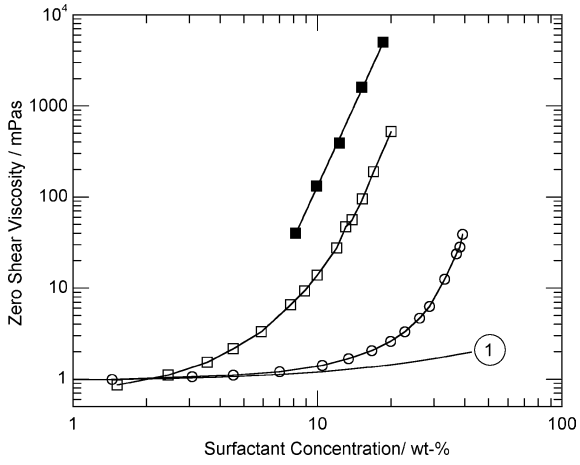


**Fig. 3** Zero-shear viscosity as a function of surfactant concentration for $C_{14}G_2$ in $D_2O$ (*filled squares*), in $H_2O$ (*open squares*) at 35 °C and $C_{12}G_2$ in $H_2O$ (*open circles*) at 22 °C. The *solid thicker line* denoted 1 is based on Einstein's equation for hard spheres at 22 °C

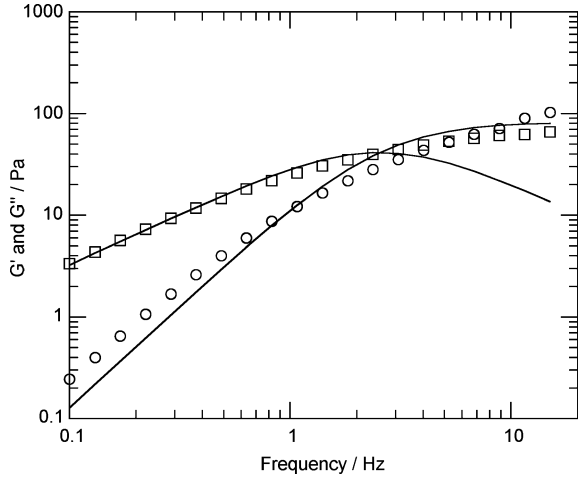


**Fig. 2** The storage modulus G' (*circles*) and the loss modulus G'' (*squares*) as a function of the frequency for a solution of 18.5 wt% $C_{14}G_2$ in $D_2O$ at 35 °C. The *solid lines* are least-squares fits of the Maxwell model

their rheological behaviour has been explained in terms of a pronounced polydispersity, which gives rise to a continuous spectrum of relaxation times rather than a single, well-defined one [7]. Our rheometric data are thus consistent with the idea that $C_{14}G_2$ form worm-like micelles at high concentration, but do not provide conclusive evidence. However, viscometric data provide strong support for this idea.

From previous SANS measurements we know that $C_{14}G_2$ micelles are elongated, flexible aggregates at low concentration. If the micelles remain disconnected also at higher concentration, we would expect to observe a transition from a dilute solution of worm-like micelles at low concentrations, to a semi-dilute regime with entangled worm-like micelles at a crossover concentration $c^*$. Furthermore, we would expect the viscosity to scale with concentration with an exponent $\gamma \geq 3.5$ in the semi-dilute region. In order to verify this expectation, the behaviour of the system over the whole micellar range was investigated by viscometry.

The zero-shear viscosity of $C_{14}G_2$ solutions in $H_2O$ and $D_2O$ is plotted as a function of concentration in Fig. 3. The zero-shear viscosity at higher concentrations was determined from the Newtonian part of the flow curves. At lower concentrations the viscosity was determined by capillary viscometry due to the higher accuracy of this method for low-viscosity liquids. In this semi-dilute regime, the dependence of the viscosity on concentration follows a power law $\eta \sim c^{\gamma}$ (Fig. 3). The exponent $\gamma$ (Table 1) is approximately the same for both $D_2O$ and $H_2O$ (namely 5.8 and 5.7, respectively), but the viscosity of $D_2O$ solutions is one order of magnitude higher. The large numeric value of $\gamma$ is not consistent with the existence of a micellar network and provides strong evidence that the micelles are worm-like. The crossover concentration $c^*$ is well-defined in solutions of "classical" polymers, where the polymers have a narrow size distribution independent of concentration. However, for "living polymers" the large size distribution and its dependence on concentration often makes it considerably less distinct [34]. The crossover region for the $C_{14}G_2$ system is quite broad, but allows for a rough estimate of $c^*$ (Table 1). The onset of the semi-dilute regime occurs at lower concentrations for $D_2O$ solutions compared with $H_2O$ ones, even when taking the density difference between $D_2O$ and $H_2O$ into account. This is

**Table 1** Data from viscometric characterisation of aqueous solutions of alkylglycosides

| Surfactant | $\delta$ | Solvent | $c^*$ (wt%) | $\gamma^a$ | $\gamma^b$ | $\gamma^c$ |
|---|---|---|---|---|---|---|
| $C_{14}G_2$ | | $D_2O$ | 4 | 5.8 | 5.8 | 5.8 |
| $C_{14}G_2$ | | $H_2O$ | 7 | 5.7 | 5.5 | 5.6 |
| $C_{12}G_2$ | | $H_2O$ | 20 | 5.6 | 5.3 | 5.4 |
| $C_9G_1$ | | $D_2O$ | 2.5 | 2.0 | 2.0 | |
| $C_9G_1$ | | $H_2O$ | 4 | 2.4 | 2.3 | |
| $C_9G_1/C_{10}G_1$ | 0.75 | $H_2O$ | 2.5 | 2.0 | | |
| $C_9G_1/C_{10}G_1$ | 0.25 | $H_2O$ | 1 | 1.6 | | |
| $C_9G_1/C_{10}G_1$ | 0.126 | $H_2O$ | – | 1.3 | | |

$\delta$ denotes the weight ratio of $C_9G_1$ in $C_9G_1/C_{10}G_1$ mixtures, $c^*$ the overlap concentration and $\gamma$ the power law growth exponent. For solutions of $C_{14}G_2$ in $D_2O$, $c^*$ was determined by extrapolation

[a]Determined as $\eta \sim c^{\gamma}$, where $c$ is the concentration expressed as wt%

[b]Determined as $\eta \sim \phi^{\gamma}$, where $\phi$ is the volume fraction assuming no water of hydration

[c]Determined as $\eta \sim \phi^{\gamma}$, where $\phi$ is the volume fraction assuming ten water molecules of hydration for each surfactant molecule

consistent with the idea that the micelles are longer in $D_2O$ than in $H_2O$. The same holds true for the observation that the viscosity is higher in $D_2O$ than in $H_2O$ for a given surfactant concentration, although the scaling exponent is largely unaffected by the deuterium exchange. This means that deuterium exchange in the $C_{14}G_2$ system induces one-dimensional micellar growth. The possible reasons for this effect have been discussed at length elsewhere [19, 23, 28]. In short, the most plausible explanation seems to be that the O–D bond is shorter than the O–H bond. Therefore, the effective area of the surfactant head-group is expected to be smaller in $D_2O$ than in $H_2O$, which, in turn, means that highly curved structures such as micellar end-caps are disfavoured.

Figure 3 displays the concentration dependence of the zero-shear viscosity of $C_{12}G_2$ in $H_2O$. For this system, the crossover concentration is ca 20 wt%, i.e. significantly higher than for $C_{14}G_2$ (Table 1). This is in agreement with previous results, which show that the micelle morphology of $C_{12}G_2$ in dilute solution shows little concentration dependence and is roughly spherical [35]. Solutions containing spherical micelles generally exhibit Newtonian behaviour and the viscosity of the solution increases linearly with the volume fraction of the micellar solution. As displayed in Fig. 3, this applies also to $C_{12}G_2$ at low concentrations. However, at higher concentrations the viscosity follows a power law with the exponent of 5.6 until the hexagonal phase is formed at 48 wt% (Fig. 3). The numerical value of the exponent is virtually identical to that for $C_{14}G_2$ and therefore provides strong evidence that also $C_{12}G_2$ forms worm-like, non-branched micelles at high concentration. This is also in agreement with the phase diagram, in which the micellar phase is followed by a hexagonal phase, rather than a phase comprising branched aggregates, upon increasing surfactant concentration.

The $\gamma$ exponents for $C_{14}G_2$ and $C_{12}G_2$ systems (Table 1) is considerably higher than what is predicted from Cates' modified reptation model for an entangled system in which the dominant relaxation mechanism is micellar scission and reformation. Rather, the data are in good agreement with the prediction for a system in which reptation dominates, cf. Eq. 2. Consequently, the data suggest that the characteristic time of micellar scission and reformation in the $C_{12}G_2$ and $C_{14}G_2$ systems is long relative to the reptation time. However, it would be highly unusual for the rheological behaviour of a micellar solution to be governed mainly by reptation, since the scission of worm-like micelles normally is so fast that it dominates the relaxation. It has to be remembered that a large numeric value of the $\gamma$ exponent may also have other grounds than sluggish micellar scission. It has previously been shown that the growth exponent $\alpha$ that governs the growth of the micelles with increasing concentration ($\bar{L} \sim \phi^{\alpha}$) can be considerably larger than the value of 0.5 given by mean field theory. For instance, the concentration-induced micellar growth of $C_{16}E_6$ in $D_2O$ has been found to be characterized by $\alpha = 1.2$. Increasing $\alpha$ leads to increasing $\gamma$, so the mean field predictions should be used with considerable caution when analysing rheological behaviour in terms of micellar dynamics [36]. A second parameter that needs to be taken into account is the influence of micellar length at a given concentration. The micelle breaking time has been found to be given by $\tau_{br} = (k\bar{L})^{-1}$, where $k$ is the temperature-dependent rate constant per unit arc length per unit time, which is independent of time and of volume fraction [29]. Consequently, shorter micelles are expected to have longer breaking time, and the fact that the $\gamma$ exponent for $C_{12}G_2$ and $C_{14}G_2$ solutions is higher than for ionic surfactants at high salt concentration can therefore be an effect of a shorter average micelle length in the former case. However, all things considered, we may with reasonable confidence conclude that our data verify the presence of worm-like, non-branched micelles in the $C_{12}G_2$ and $C_{14}G_2$ systems.

For typical polymer solutions, the viscosity is a weak function of temperature. In contrast, the viscosity of solutions of "living polymers" often shows a strong, Arrhenius-like temperature dependence that has been interpreted as an effect of the decrease in average micellar length upon increasing temperature [37]. This picture is not directly applicable to the $C_{14}G_2$, for which previous data show an increase in micellar size with temperature [23]. For $C_{12}G_2$ and $C_{14}G_2$, we rather find that the viscosity increases with increasing temperature, and that the increase is not of Arrhenius-type (data not shown).

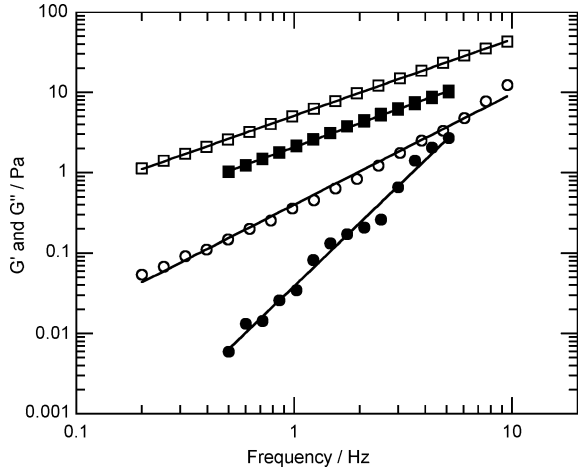


**Fig. 4** The storage modulus G' (*circles*) and the loss modulus G'' (*squares*) as a function of the frequency for a solution of 55 wt% $C_9G_1$ in $D_2O$ (*open symbols*) and 42.5 wt% $C_9G_1$ in $D_2O$ (*filled symbols*) at 22 °C. For the latter system, the data represent the mean value of three independent measurements. The *straight lines* are least-square fits to the data

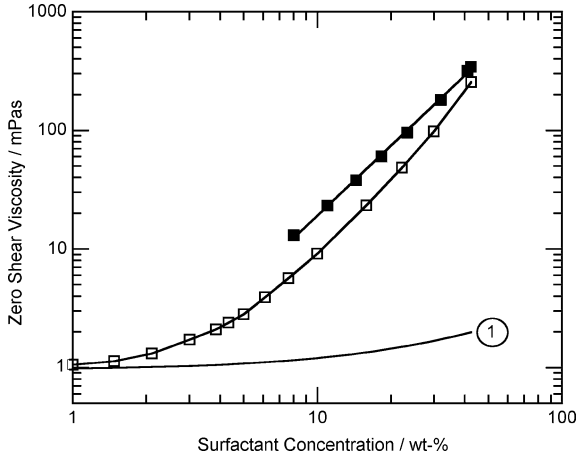


**Fig. 5** The zero-shear viscosity as a function of surfactant concentration for $C_9G_1$ in $D_2O$ (*filled squares*) and $C_9G_1$ in $H_2O$ (*open squares*) at 22 °C. The *solid thicker line* denoted 1 is based on Einstein's equation for hard spheres

## Nonylglucoside, $C_9G_1$

The viscosity as a function of shear rate was investigated for $C_9G_1$ in $D_2O$ and $H_2O$ (Fig. 1). As is obvious from the figure, the rheological behaviour of $C_9G_1$ is quite different from that of $C_{14}G_2$. In particular, the viscosity of $C_9G_1$ solutions is dramatically lower than for $C_{14}G_2$ for comparable concentrations. Furthermore, $C_{14}G_2$ solutions display shear thinning, whereas the viscosity of $C_9G_1$ is independent of shear rate over the entire range investigated (0.1–785 $s^{-1}$). Measurements with oscillating rheology confirm the pronounced differences between $C_9G_1$ and the maltosides. The viscoelasticity of $C_9G_1$ solutions is comparably weak, and the relaxation is so fast that no crossover point can be determined in the frequency spectrum (Fig. 4). Detailed, further analysis of the frequency spectrum in terms of the Maxwell model or any other mechanical description is not possible. However, the fact that the characteristic time of the $C_9G_1$ system is much shorter than that of the $C_{14}G_2$ system clearly suggest a pronounced difference in aggregation between the two surfactants.

In Fig. 5, the zero-shear viscosity for $C_9G_1$ in $D_2O$ and $H_2O$ is presented as a function of concentration. For $C_9G_1$ in both $D_2O$ and $H_2O$, the viscosity scales with concentration with an exponent considerably lower than for the alkylmaltosides (Table 1). The exponent is also lower than predicted by theory if the relaxation mechanism would be determined by scission and recombination of the micelles. Other relaxation mechanisms could, in principle, give rise to exponents as low as 2.0 for worm-like micelles [32]. However, it would seem exceedingly difficult to explain the pronounced differences in rheological and viscometric behaviour between $C_9G_1$ and the maltosides while assuming worm-like micelles in both cases. Rather, the low numerical value of the exponent for $C_9G_1$ may be considered indicative of branched aggregates. This explanation is in full agreement with the phase behaviour of the surfactants. As described above, the micellar phase of $C_9G_1$ is followed by a bicontinuous cubic phase of *Ia3d*-type at temperatures above 11 °C. NMR self-diffusion data across the phase boundary between the cubic and the micellar phase shows no discontinuity, which suggest that the microstructure in the two phases is similar [18]. For the $C_{12}G_2$ and (presumably) the $C_{14}G_2$ systems, on the other hand, the micellar phase is followed by a hexagonal phase.

The effect of deuterium exchange on the viscosity is much smaller for $C_9G_1$ than for the maltoside $C_{14}G_2$ (Table 1). On the other hand, the effect on the scale factor is larger and leads to a smaller scale factor in $D_2O$ solution. This deuterium effect would be compatible with a decrease in the number of dead ends in an interconnected micellar network.

In Fig. 6 the relative viscosity of a 28 wt% solution of $C_9G_1$ in $D_2O$ is plotted as a function of the inverse temperature. Upon increasing temperature the viscosity decreases and the relation between viscosity and inverse temperature is perfectly linear. This Arrhenius-like behaviour again sets $C_9G_1$ apart from the maltosides. From the slope of the plot, we can calculate the activation energy $E_a$ to 32 kJ/mol. This value is relatively low when compared with those previously reported for ionic micelles that form entangled networks of worm-like micelles (70–300 kJ/mol) [11]. However, as branching occurs the activation energy is often lowered [1, 10] and the low activation energy in the $C_9G_1$ system may

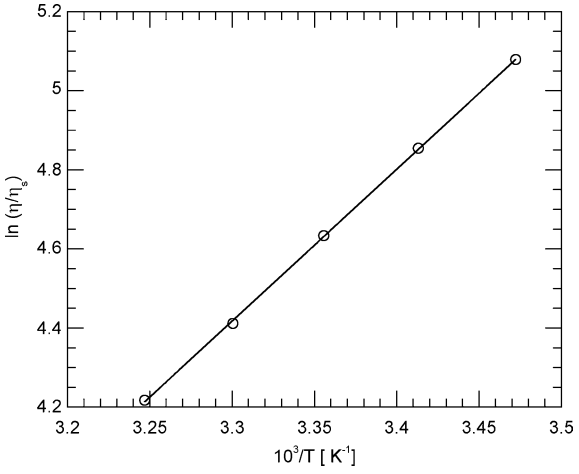


**Fig. 6** Semi-logarithmic representation of relative viscosity ($\eta/\eta_s$) versus $10^3/T$ for 28 wt% $C_9G_1$ in $D_2O$. The *straight line* is the best least-square fit to the data

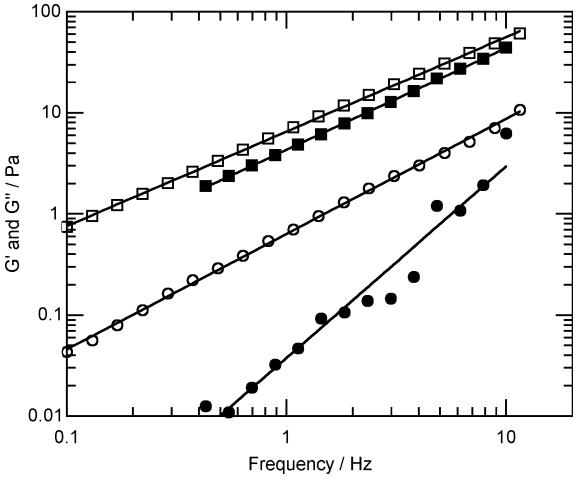


**Fig. 7** The storage modulus G' (*circles*) and the loss modulus G'' (*squares*) as a function of the frequency for a solution of 50 wt% $C_{10}G_1$ in $D_2O$ (*open symbols*) at 25 °C and 45 wt% $C_9G_1/C_{10}G_1$ $\delta = 0.25$ in $H_2O$ (*filled symbols*) at 22 °C. For the latter system, the data represent the mean value of two independent measurements. The *straight lines* are least-square fits to the data

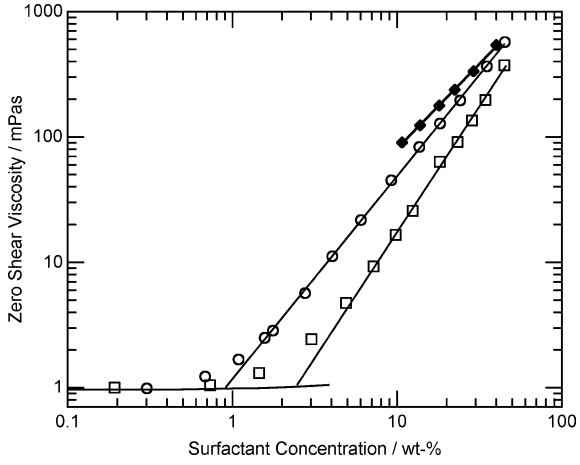


**Fig. 8** The zero-shear viscosity as a function of surfactant concentration for mixtures of $C_9G_1$ and $C_{10}G_1$ in $H_2O$ with $\delta = 0.75$ (*open squares*) $\delta = 0.25$ (*open circles*) and $\delta = 0.126$ (*filled diamonds*). For the system with $\delta = 0.126$, measurements at lower concentration are made impossible by the phase separation of the system to two micellar phases (see Introduction)

therefore act as further evidence for the presence of inter-micellar connections in this system.

## Mixtures of nonyl- and decylglucoside, $C_9G_1/C_{10}G_1$

Due to the phase separation that dominates the micellar domain of the $C_{10}G_1$/water phase diagram, it is not meaningful to determine a scaling factor for the viscosity-concentration power law. However, rheological data show that concentrated solutions of $C_{10}G_1$ behave similarly to $C_9G_1$ (Fig. 7). Nevertheless, for comparable (molar) concentrations, the frequency spectra suggest that the relaxation time is even shorter for the $C_{10}G_1$ system. This lends some support to the assumption that $C_{10}G_1$ forms a network that contains less end-points than that formed by $C_9G_1$. Measurements on $C_9G_1/C_{10}G_1$ mixtures substantiate this idea. Capillary viscometry measurements were performed along three dilution lines ($\delta = 0.75$, 0.25 and 0.126) in the ternary $C_9G_1/C_{10}G_1$/water phase diagram. As outlined in the Introduction, the phase behaviour of this system has been described in terms of a formation of an interconnected micellar network, the end-points of which increase in number with the $C_9G_1$ ratio. As can be seen in Fig. 8 and Table 1, $\gamma$ decreases from 2.0 to 1.3 with increasing ratio of $C_{10}G_1$, which is clearly compatible with the suggested change of micellar properties. It is also interesting to note that the limiting scale factor for network-forming PEG-based surfactants has been reported to be 1.3 [13]. From Fig. 8 and Table 1 it can be seen that the overlap concentration $c^*$ is also decreasing with increasing ratio of $C_{10}G_1$, which indicates earlier onset of network formation. This is consistent with previous fluorescence quenching measurement that show $C_{10}G_1$ to form larger aggregates than $C_9G_1$ [18]. The overlap concentration is also observed to be more distinct as the ratio of $C_{10}G_1$ is increased, which is again consistent with the idea that formation of micellar cross-links become more important than micellar scission for the viscosity of systems rich in $C_{10}G_1$. The frequency spectrum (Fig. 7) lends some support to this idea in the sense that the relaxation time (as roughly estimated from the slopes) is suggested to decrease in the sequence $C_9G_1 > C_9G_1/C_{10}G_1 > C_{10}G_1$. In quite general terms, the

viscometric and rheological data are therefore compatible with the notion that increased packing parameter of the glycosides (going from $C_9G_1$ to $C_{10}G_1$) gives rise to a transition from a branched, interconnected micellar system to a proper, space-filling micellar network.

## Conclusion

The rheological properties of the maltoside and glucoside solutions investigated in the present work show similarities with those previously reported for ionic surfactants forming worm-like micelles and interconnected micellar networks. For the maltosides $C_{12}G_2$ and $C_{14}G_2$, we find that the rheological and viscometric data are consistent with the idea that these surfactants form entangled networks of polydisperse, worm-like micelles. Substituting $D_2O$ for $H_2O$ increases the viscosity of $C_{14}G_2$ solutions by one order of magnitude, without appreciably affecting the scale factor in the viscosity-concentration power law. This clearly suggests that the deuterium exchange induces one-dimensional micellar growth, in agreement with previous data.

The rheological behaviour of solutions comprising the glucosides $C_9G_1$ and $C_{10}G_1$ is strikingly different from that of the maltosides. Here, the scale factor is much lower than predicted for micellar systems in which micellar scission and reptation are the two main relaxation mechanisms. Indeed, for $C_{10}G_1$-rich mixtures of the two surfactants, the scale factor approaches unity and is therefore entirely inconsistent with the predicted properties of an entangled micellar network. Rather, the data verify and substantiate the notion that these surfactants, as well as their mixtures, form interconnected micellar networks. Nevertheless, there are differences in rheological behaviour between the $C_9G_1$ and $C_{10}G_1$ systems. These differences are possible to account for by assuming that the number of dead ends is larger in the $C_9G_1$ network than in the $C_{10}G_1$ one. The effect of deuterium exchange on the viscosity is much smaller for $C_9G_1$ than for the maltoside $C_{14}G_2$. On the other hand, the effect on the scale factor is larger and leads to a smaller scale factor in $D_2O$ solution. This would seem to suggest that the deuterium effect in this case amounts to a decrease in the number of dead ends in the interconnected micellar network.

**Acknowledgments** This research has been funded by the Centre of Competence for Surfactants Based on Natural Products (SNAP) an AstraZeneca R&D Lund.

## References

1. Khatory A, Kern F, Lequeux F, Appell J, Porte G, Morie N, Ott A, Urbach W (1993) Langmuir 9:933
2. Appell J, Porte G, Khatory A, Kern F, Candau SJ (1992) J Phys II France 2:1045
3. Candau SJ, Khatory A, Lequeux F, Kern F (1993) J Phys IV 3:197
4. Candau SJ, Hirsch E, Zana R, Delsanti M (1989) Langmuir 5:1225
5. Khatory A, Lequeux F, Kern F, Candau SJ (1993) Langmuir 9:1456
6. Kern F, Lemarechal P, Candau SJ, Cates ME (1992) Langmuir 8:437
7. Rehage H, Hoffmann, H (1988) J Phys Chem 92:4712
8. Harwigsson I, Söderman O, Regev O (1994) Langmuir 10:4731
9. Monduzzi M, Olsson U, Söderman O (1993) Langmuir 9:2914
10. Croce V, Cosgrove T, Maitland G, Hughes T, Karlsson G (2003) Langmuir 19:8536
11. Raghavan SR, Kaler EW (2001) Langmuir 17:300
12. Lequeux F (1992) Europhys Lett 19:675
13. Kato T, Terao T, Seimiya T (1994) Langmuir 10:4468
14. Imae T, Sasaki M, Ikeda S (1989) J Colloid Interface Sci 127:511
15. Bryskhe K (2004) Physical chemistry 1, Lund University
16. Häntzschel D, Schulte J, Enders S, Quitzsch K (1999) Phys Chem Chem Phys 1:895
17. Schulte J, Enders S, Quitzsch K (1999) Colloid Polym Sci 277:827
18. Nilsson F, Söderman O, Hansson P, Johansson I (1998) Langmuir 14:4050
19. Ericsson CA, Söderman O, Garamus VM, Bergström M, Ulvenlund S (2004) Langmuir 20:1401
20. Nilsson F, Söderman O, Reimer J (1998) Langmuir 14:6396
21. Whiddon CR, Söderman O, Hansson P (2002) Langmuir 18:4610
22. Whiddon CR, Reimer J, Söderman O (2004) Langmuir 20:2172
23. Ericsson CA, Söderman O, Garamus VM, Bergström M, Ulvenlund S (2005) Langmuir 21:1507
24. Cecutti C, Focher B, Perly B, Zemb T (1991) Langmuir 7:2580
25. He L-Z, Garamus VM, Funari SS, Malfois M, Willumeit R, Niemeyer B (2002) J Phys Chem B 106:7596
26. Boyd BJ, Drummond CJ, Krodkiewska I, Grieser F (2000) Langmuir 16:7359
27. Auvray X, Petipas C, Dupuy C, Louvet S, Anthore R, Rico-Lattes I, Lattes A (2001) Eur Phys J E 4:489
28. Whiddon CR, Söderman O (2001) Langmuir 17:1803
29. Cates ME (1987) Macromolecules 20:2289
30. Cates ME (1990) J Phys Chem 94:371
31. Cates ME, Candau SJ (1990) J Phys Condens Matter 2:6869
32. Hassan PA, Candau SJ, Kern F, Manohar C (1998) Langmuir 14:6025
33. Drye TJ, Cates ME (1992) J Chem Phys 96:1367
34. Carale TR, Blankschtein D (1992) J Phys Chem B 96:459
35. Focher B, Savelli G, Torri G, Vecchio G, McKenzie DC, Nicoli DF, Bunton CA (1989) Chem Phys Lett 158:491
36. Schurtenberger P, Cavaco C, Tiberg F, Regev O (1996) Langmuir 12:2894
37. Magid LJ (1998) J Phys Chem B 102:4064